Renewable and Sustainable Energy Reviews 29 (2014) 865–882

Contents lists available at ScienceDirect

Renewable and Sustainable Energy Reviews

journal homepage: www.elsevier.com/locate/rser

Comparison of the performance of compressed-air and hydrogen energy storage systems: Karpathos island case study

S. Karellas*, N. Tzouganatos

National Technical University of Athens, Laboratory of Steam Boilers and Thermal Plants, School of Mechanical Engineering, 9 Heroon Polytechniou, 15780 Zografou, Athens, Greece

ARTICLE INFO

Article history:
Received 6 December 2011
Received in revised form
9 July 2013
Accepted 14 July 2013
Available online 2 October 2013

Keywords:
Compressed air energy storage (CAES)
Hydrogen storage
Performance evaluation
Karpathos island

ABSTRACT

Two diverse energy storage technologies, namely the compressed-air and hydrogen energy storage systems, are examined. In particular, a steady state analysis (IPSEpro simulation software) of four configurations of micro-CAES systems is conducted from the energetic and exergetic point of view. The hydrogen energy storage system is dynamically simulated using the HOMER energy software. Load and wind profiles for the island of Karpathos are used as input data to the program. The two-stage micro-CAES system without air preheating is selected to be investigated dynamically as it is proven to have high efficiency and zero emissions. The last part of the paper compares the two systems in terms of energy storage efficiency, includes an approximation of the costs and highlights the technological advantages and disadvantages of these technologies.

Contents

1. Introduction . . . 866
2. Compressed air energy storage (CAES) . . . 866
   2.1. Conventional CAES . . . 866
   2.2. AA-CAES . . . 867
   2.3. ISobaric Adiabatic COmpressed Air energy STorage with Combined Cycle (ISACOAST-CC) project . . . 868
3. Micro-Compressed air energy storage (micro-CAES) . . . 869
4. Hydrogen energy storage . . . 869
5. Simulation of a micro-CAES system using IPSE-pro software . . . 870
   5.1. Systems and main assumptions . . . 870
   5.2. Energetic analysis . . . 871
   5.3. Exergetic analysis . . . 872
   5.4. Results and discussion . . . 872
6. Simulation of an energy–hydrogen storage hybrid power generation system . . . 873
   6.1. Input data . . . 873
   6.2. Input variables . . . 873
      6.2.1. Wind turbines . . . 873
      6.2.2. Electrolyzing unit . . . 873
      6.2.3. Hydrogen storage tank . . . 874
      6.2.4. Fuel cell . . . 874
      6.2.5. System requirements . . . 874
   6.3. Results and discussion . . . 874
7. Dynamic analysis of the compressed air energy storage system and comparison to the hybrid energy–hydrogen storage power generation system . . . 876
   7.1. Dynamic analysis of the CAES system . . . 876
      7.1.1. Input variables . . . 876
      7.1.2. Compressor unit . . . 876

* Corresponding author. Tel.: +30 210 7722720; fax: +30 210 7723663.
E-mail address: sotokar@mail.ntua.gr (S. Karellas)

1364-0321/$ - see front matter © 2013 Elsevier Ltd. All rights reserved.
http://dx.doi.org/10.1016/j.rser.2013.07.019

7.1.3. Compressed air storage tank . . . 876
7.1.4. Expansion unit . . . 877
7.1.5. System requirements . . . 877
7.1.6. Results and discussion . . . 877
7.2. Comparison of the compressed air energy storage system to the hybrid energy–hydrogen storage power generation system . . . 878
7.2.1. Efficiency . . . 878
7.2.2. Costs . . . 879
8. Conclusions . . . 880
References . . . 881

1. Introduction

The increasing world energy demand along with the predicted abrupt escalation in oil prices and the need to curb greenhouse gas emissions resulted in a remarkable growth of electricity generated from renewable energy sources (RES). However, the introduction of these fluctuating energy sources brings about important network stability problems due to a supply–demand imbalance and makes the need for energy storage more demanding than ever before. And this problem is getting worse when it comes to decentralized electricity production.

As far as Greece is concerned, the problem consists of two major components: (a) the presence of many islands with no electricity transfer possibilities and (b) the abrupt increase of the electrical load during the high season. Specifically, as RES fluctuate independently from electricity demand, there will be times when the unmet load should be met by a conventional plant. As a result, and in order to satisfy 100% of the electricity needed through RES, energy storage is required [1]. Development of storage methods will open up a new field of application, especially due to the growth of electrical production from renewable energy, along with decentralized production.

Aim of this work is the investigation – from the steady-state and dynamic point of view – and comparison of two energy storage methods: energy storage by means of compressed air and hydrogen (H_2), which are applied in a community of the Greek island Karpathos.

2. Compressed air energy storage (CAES)

Compressed air energy storage is a promising method of energy storage due to its high efficiency and the fact that it relies on mature technology with several projects in place. Currently, there are two conventional CAES plants operating (Neuenhuntorf [2] and McIntosh), while two more plants are under construction (Norton and Iowa [3]) [4–7]). As far as AA-CAES plants (adiabatic compressed air storage systems) are concerned, industrial applications are expected approximately in 2015. The construction of the pilot project of EnBW AG is expected to be completed in 2013, but at the first stage it will be operated as a conventional air storage plant and at the second stage as an AA-CAES with overall efficiency of about 70% and capacity ranging from 150 to 600 MW [4].

2.1. Conventional CAES

The operation of a conventional compressed air energy storage system is described as follows: excess electricity during off-peak hours is used to drive a 2-stage compressor with intercooling. After the compression, the compressed air (40–70 bar) is led to an after-cooler before it gets stored in an underground storage reservoir. At peak hours, a combustion chamber is employed in order to heat-up stored air and, as a result, to obtain increased power during the expansion process (expansion with reheating). The operating principle of the Neuenhuntorf CAES plant [7] is presented in Fig. 1.

In modern systems, a recuperator is also used in order to preheat the stored compressed air before it enters the combustion chamber. This way, the efficiency of the system is increased by 10%. However, a significant drawback of this configuration is the big size of the recuperator, which implies an increase in the investment costs of the plant [1]. The CAES plants at McIntosh and Neuenhuntorf represent the two options of operating a conventional power plant (with and without the use of a recuperator respectively) [7]. The operating principles of the McIntosh plant are presented in Fig. 2.

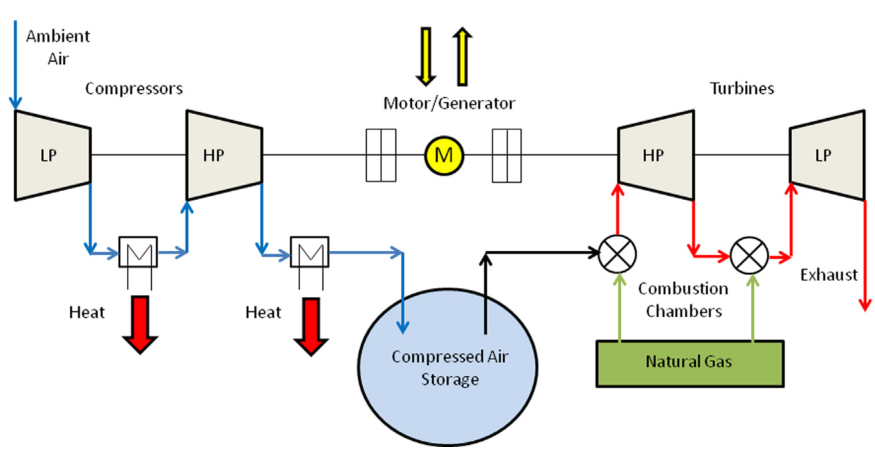


Fig. 1. Operating principle of the CAES plant Neuenhuntorf.

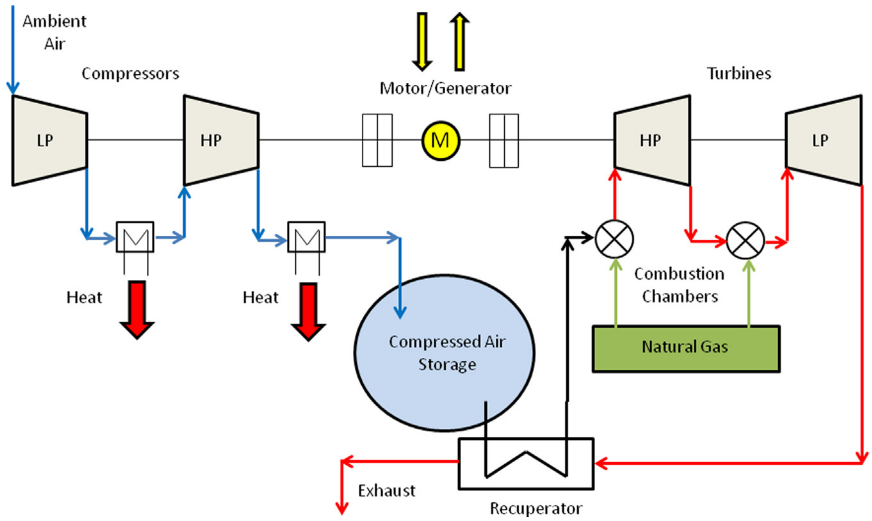


Fig. 2. Operating principle of the McIntosh CAES plant.

Referring to the components of a CAES power plant: The incoming air is compressed either by axial compressors with a pressure ratio of about 20 and a flow rate of 1.4 Mm^3/h or by radial compressors with flow rates up to 100,000 m^3/h and capable of increasing the pressure up to 1000 bar. At the current level of technology, air compression is performed in two stages with intercooling at temperatures ranging from 40 to 200 °C [5].

High pressure air–fuel mixture is expanded in air turbines with pressure ratios up to 22 and with a maximum inlet temperature of 1230 °C. As Nölke reported in [5], comparative studies have shown that the best choice for the expansion sector of a CAES power plant is the use of a turbine consisting of two parts: a common air turbine part and a steam turbine as the high pressure turbine.

Compressed air is stored at near-ambient temperature conditions that allow higher density of the stored medium and reduced size of the storage reservoir. The aquifer, underground caverns made of high quality rocks, depleted natural gas storage caves and salt domes with storage capacities of 300,000 to 600,000 m^3 are most commonly used for the compressed air storage. Storage in underground, high-pressure pipes (20–100 bar) has also been shown to be a feasible alternative.

Compressed air energy storage has been extensively studied in terms of system performance, operation scheduling, integration to the power transmission grid and different configurations for the storage of compressed air. Oldenburg and Pan [8] studied the suitability of porous media systems (e.g. aquifers and depleted hydrocarbon reservoirs) for large scale energy storage and calculated their efficiency by modeling a prototypical wellbore-reservoir system. Ibrahim et al. [9] investigated different technical alternatives for coupling compressed air energy storage to wind–diesel hybrid systems. Abbaspour et al. [10] proposed an optimal operation schedule of a CAES system by modeling two objective functions (profit maximization and cost minimization), while Lund et al. [11] focused their research activities on defining an optimal operation strategy based on electricity spot markets with fluctuating prices. The energy-balance effect of adding a CAES system to the Western Danish energy system and its ability to eliminate excess electricity production from wind power was analyzed by Salgi and Lund [12]. Novel system configurations have been proposed such as the one combining compressed air energy storage with pumped hydro technology [13] in an attempt to replace the water dam.

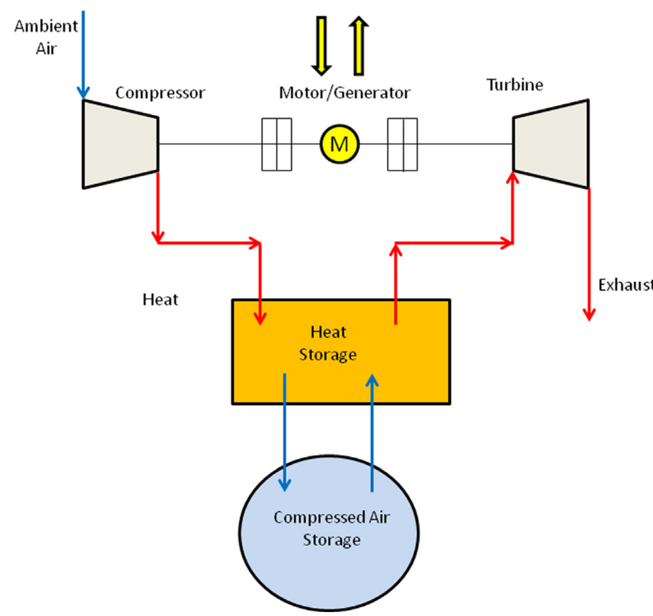


Fig. 3. Operating principle of the AA-CAES system.

2.2. AA-CAES

The main difference of AA-CAES to conventional CAES systems is the additional storage of the heat released during compression in a separate heat storage reservoir. The idea of developing such a system reaches back to the 1980s, but no plant was developed due to technological barriers. The interest for the development of AA-CAES plants was reignited by the increasing fuel prices and the need to reduce CO_2 emissions.

The operating principle of an AA-CAES system is shown in Fig. 3. Air is compressed without intercooling and releases its heat in a separate heat storage reservoir before being stored. At discharge periods, compressed air is heated up to the appropriate turbine inlet temperature (~600 °C) by regaining the heat from the heat storage reservoir. Overall efficiency rates of adiabatic compressed air storage plants are expected to reach values up to 70% [4,5,7].

In two-stage AA-CAES systems, heat released in the low (LP) and high-pressure (HP) compressors is stored in separate heat tanks. At discharge periods, heat from the HP and LP heat tanks is

regained before the inlet to the HP and LP turbines, respectively. Two-stage AA-CAES systems achieve higher energy storage density, which compensates for the increased complexity of the plant (two heat storage tanks and piping).

A thermodynamic analysis of the design parameters of multi-stage adiabatic CAES systems and their influence on the system efficiency, and mainly on the heat transfer apparatus, has been performed by Grazzini and Milazzo [14]. The thermodynamic effect of thermal energy storage on AA-CAES systems has been investigated in [15], while the air storage chamber model selected for the simulation of the charge and discharge processes was shown to have an important effect on the performance and the working stability of the system [16].

Important advantages of the AA-CAES technology are the elimination of the fuel added before expansion in the turbine and of the concomitant CO_2 emissions, as well as the compression of air without intercooling that allows for higher outlet temperatures from the compressor and, thus, higher amounts of heat stored in the heat tank. However, major components of the plant need to be redesigned as conventional ones cannot be utilized. Specifically, heat storage tanks with capacities of 120–1800 MWh_{th}, need special design to achieve sufficiently high heat transfer rates and constant outlet temperature. Minimization of heat losses during charging and discharging of the heat reservoir is another point of consideration [17–19].

Referring to the compressor of the plant, in AA-CAES systems adiabatic compression is preferred to isothermal - which is adopted in conventional CAES plants. However, conventional compressors can not reach the high pressures and temperatures required for adiabatic compression (100 bar/620 °C for single-stage and 160bar/450°C for two-stage AA-CAES plants) and, along with the need for low response times and high isentropic efficiency, the design of novel compressors for AA-CAES systems becomes a necessity. Recent studies converge that the satisfaction of these requirements is best achieved by constructing a compressor consisting of three parts: (a) an axial or a radial compressor as the low pressure compressor in case of high or low air flow rates, respectively, and single-shaft radial compressors for the (b) intermediate and (c) high pressure sectors.

The turbine sector needs to be redesigned to achieve increased turbine inlet temperatures, air flow rates and efficiency. In order to satisfy these requirements, a novel non-conventional regulation stage with lower losses should be designed for improved handling of pressure and flow rate fluctuations. Pre-heating of the turbine is also proved to be desirable in order to achieve temperature profiles, which will enable low response times [17–19].

2.3. ISobaric Adiabatic COmpressed Air energy STorage with Combined Cycle (ISACOAST-CC) project

An innovative compressed air energy storage research initiative by E.ON AG is currently developed with the support of the Institute WBT of the Technical University Braunschweig and the Institute RuS of the Ruhr-University of Bochum. The main concept of this research initiative lies on the combination of the CAES and the AA-CAES processes and their advantages by employing both a combustion chamber (CAES concept) and a heat storage tank (AA-CAES concept). However, a component that is neither a part of the CAES project nor of the AA-CAES is used for the realization of this new research initiative, namely a brine shuttle bond at the earth surface to enable the storage of the compressed air at nearly constant pressure [20,21].

The operating principles of the ISACOAST-CC plant is shown in Fig. 4. Air is compressed without intercooling during hours of wind energy production surplus. Before being stored in the cavern at around 50 °C (temperature limit due to negative effects on the stored air mass and the stability of the cavern), the compressed air flows through the heat storage tanks where it releases the compression waste heat. The heat is initially transferred to the helically-shaped steel tubes inside the tanks at high pressure and, finally, to the storage material at atmospheric pressure. The cool air stream is driven to the storage caverns, where it forces the enclosed brine to the brine shuttle bond (nearly isobaric process). At insufficient wind energy production, the caverns are discharged and filled with brine, while the compressed air flows through the heat storage tank to regain the stored heat before entering the combustion chambers. In specific, the air is heated up to a temperature that is slightly lower than the compressor outlet temperature. The hot air stream enters the combustion chambers, where it is heated up to about 1400 °C, and the exhaust gases drive the gas turbines coupled to the generators and electric power is produced. Finally, the gases leaving the gas turbine at about

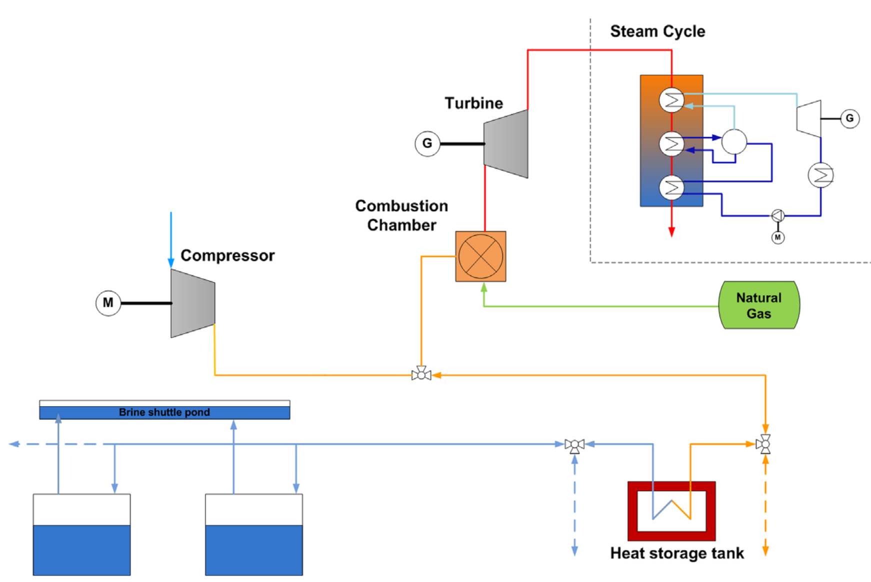


Fig. 4. Operating principle of the ISACOAST-CC plant.

Table 1
Main components of the ISACOAST-CC plant [12].

Component	Technical characteristics
Storage caverns	Capacity: 2,400,000 m^3 (16 × 150,000 m^3)
Heat storage unit	8 storage tanks
	Diameter and height: 30 m
	Total storage capacity: 20 GWh
Compressors	2 × Alstom GT 26
Gas Turbines	2 × Alstom GT 26 (CC)
Brine shuttle	Surface area: 480,000 m^2
Pond	Height fluctuation: 5 m

500–600 °C are used as the heat source of a steam cycle in order to vaporize water and produce additional electricity [20,22]. Table 1 summarizes the main components of the plant and their technical characteristics [21].

This new research initiative combines concepts and advantages of the conventional and adiabatic compressed air storage concepts as well as newly developed components (e.g. quasi-isobaric air storage cavern) in order to achieve increased efficiency (values around 80% seem to be realistic). Specifically, the storage efficiency is increased due to the storage and utilization of the compressor waste heat, while the constant high turbine inlet temperature allows for a constant power output during the discharge mode. The option of natural gas co-firing results in doubling the stored electricity. The ISACOAST-CC project further presents significantly higher specific storage capacity (> 16 kWh/m^3) compared to the conventional plants (1.93 kWh/m^3 (Huntorf)) due to the utilization of the total air amount stored in the cavern. A further advantage of the plant is that modified standardized gas and steam power plants with high efficiencies can be employed for the realization of the project. This way the plant can operate as a conventional combined cycle power plant without the use of the air and heat storage systems in order to produce peak-load electricity, which results in the improvement of its economic viability. The reduced mechanical stresses in the cavern due to the low variation of the turbine inlet pressure and temperature results in higher lifetime and stability of the cavern. Finally, the plant is flexible at partial loads due to the decoupled turbomachine structure and the variable-speed operation of the compressor, while the axial forces in the turbomachine are compensated due to its bidirectional flow arrangement [20,21,23].

3. Micro-Compressed air energy storage (micro-CAES)

Micro-CAES systems are characterized by the fact that the compressed air is not stored in high volume underground reservoirs, but in smaller amounts over the earth surface. Thus, these plants appear to be independent from the geological characteristics of the installation area and can be installed at the best position from the technical point of view (e.g. proximity to a wind park). Generic guidelines for the pressure and the efficient design and sizing of micro-CAES pressure vessels are provided in [24]. Most of the existing micro-CAES systems have been designed in order to allow for uninterruptible power supply. Thus, reliability, operational simplicity and low response times play a crucial role for the viability of the power plant, whereas efficiency and specific production costs are of secondary importance [25].

A wide range of micro-CAES system configurations can be designed based on modifications in the compression and expansion processes. In contrast to large-scale CAES systems, where compression is commonly performed in two stages with inter-cooling, in micro-CAES systems it is crucial to keep the structure simple and simultaneously achieve high efficiency levels. Thus, compression and expansion need to be closer to isothermal than to adiabatic processes [26].

A quasi-isothermal compression can be achieved by injecting large amounts of water or liquid in the compressor for the absorption of the waste heat. After the compression process, the air-water mixture is separated and the air stream is cooled down to ambient temperature before entering the storage tank. The energy of high pressure water is recovered by a hydraulic motor and the water stream is cooled down and recirculated. For the expansion process, preheating of the air stream in a heat exchanger or a combustion chamber before the turbine inlet are not required in contrast to conventional CAES systems. Expanded air at the turbine outlet can be utilized to satisfy cooling loads in micro-CAES systems. A trigeneration system for the production of electrical, heating and cooling power for domestic households and small scale office buildings has been proposed, thermodynamically analyzed and evaluated for its performance by Li et al. [27]. For the achievement of an isothermal expansion process, water or another liquid has to be injected during expansion. The gas–liquid mixture is led to a separator after the turbine exit and the fluid is used to satisfy cooling loads, then compressed and recirculated. A quasi-isothermal expansion process can also be achieved by adding fuel or preheating the turbine by injection of high temperature liquids during the expansion process.

Generally, a micro-CAES system is characterized by high pressure ratios during compression and expansion, leading to large temperature differences and high efficiency. Referring to adiabatic process systems, there is high exergy destruction mainly caused by the high temperature differences between the beginning and the end of each process, and secondly by the low heat recovery in the hydraulic motor and the recuperator. As a result, two or more compression and expansion stages with intercooling or reheating respectively are needed in order to achieve high energetic and exergetic efficiency. In contrast to adiabatic systems, quasi-isothermal micro-CAES systems do not require the employment of a two-stage process, as the contribution of a second stage to the increase of the overall efficiency is proven to be negligible. Additionally, they minimize exergy losses and provide the opportunity to achieve the appropriate temperatures after compression and expansion through regulation of the mass flow rate, so that thermal loads can be satisfied. Thus, they are more efficient compared to other micro-CAES systems and can be applied at decentralized energy networks [26].

Micro-CAES systems for the utilization of excess electricity from wind farms have been developed and tested like SCAES (Small CAES) by Energy Storage and Power Consultants (ESPC) Inc., T-CAES (Transportable CAES) by Enis WindGen Renewable Energy Systems LLC and TACAS (Thermal and Compressed Air Energy Storage) by Active Power [28].

4. Hydrogen energy storage

Hydrogen is seen as the most promising alternative to conventional energy carriers due to its high energy density by weight, its high chemical-to-electical conversion efficiency and vice versa, and the wide range of possibilities H_2 offers in terms of transportation and storage. Specifically, the advantages of energy-hydrogen storage hybrid power generation systems are the following: (i) charge-discharge rates and storage tank capacity are independent variables, (ii) modular construction, (iii) applicability to a wide range of sizes and power outputs, and (iv) environmentally friendly operating principles [29,30]. However, significant drawbacks that should be faced before commercialization of the technology are the high costs and low efficiency (< 50%). The latter can be reduced further when Internal Combustion Engines (ICEs) or hydrogen gas turbines are

used as electricity production units in place of Fuel Cells (FCs). Currently, several pilot projects are under operation or construction such as the Utsira and ENEA parks, and the FIRST, RES2H2, PURE and HARI projects [31–33].

Energy–hydrogen storage hybrid power generation systems follow the described operating principles: During off-peak hours, excess electricity is used to feed an electrolyzer converting incoming water to hydrogen, which in turn is led to a compressor and a storage unit. If the excess of produced power is higher than the nominal power of the electrolyzing unit and regardless the level of the H_2 storage tank, this amount of electricity is rejected and can be used for other needs. On the other hand, when it comes to peak load hours, the difference between the demanded and the produced amount of electricity is supplied by utilizing stored hydrogen in fuel cells, internal combustion engines or hydrogen gas turbines.

As far as the components of a H_2 hybrid power generation plant are concerned, electrolyzing units installed in decentralized power systems should satisfy two basic requirements: (i) low start-up times and (ii) capability to operate under low partial load to allow hydrogen production even when excess electricity is low. The former can be alleviated by taking weather forecasts and load predictions into account. The only electrolyzing devices that are able to satisfy the aforementioned requirements are alkaline, advanced alkaline and Proton Exchange Membrane (PEM) electrolyzers. Alkaline electrolyzers represent a mature technology, while there is no mass production of mid- and high power PEM electrolyzers yet (available only for pilot projects with a hydrogen production rate ranging between 10 and 20 N m^3/h), leading to high investment costs. Manufacturers estimate the investment cost of alkaline electrolyzing units to drop down to 8150 €/N m^3/h with PEM units being about 30% more expensive [32,34].

Hydrogen is typically stored in its gaseous form at ~200 bar and temperatures ranging between −50 °C and 60 °C, while the mass content cannot exceed 2–3 wt%. At large H_2 amount, the use of a compressor is inevitable and this results in an increase of both the investment and O&M costs [32,35].

Liquefied hydrogen storage is also developed due to the higher energy density of liquid hydrogen. However, important drawbacks such as high energy demand for the liquefaction of hydrogen (≈30% of LHV), high complexity and cost of liquefaction plants, significant hydrogen losses due to evaporation (≈0.1% of the hydrogen content daily) and short storage times prevent the use of this storage method in the case of decentralized power systems [36–38].

The only commercially available chemical method for H_2 storage is the use of metal hydrides with low temperature H_2 desorption. However, a range of other materials are currently under R&D so that problems such as the achievement of reasonable pressure and temperature ranges during absorption and desorption processes as well as weathering of materials can be tackled. Hydrogen storage in rare earth intermetallic compounds by the use of methanol is excluded in the case of decentralized power systems as the production and reforming of these compounds are energy intensive and increase the complexity and the costs of the storage plant. Finally, hydrogen storage in carbon nanotubes -both in the inside of the tubes and in the pores on their surface- has been proposed [39–46]. Summing up, metal hydride hydrogen storage can achieve energy density (by volume) in the same order of magnitude as compressed gaseous H_2 storage while the maximum obtainable weight content can reach 0.07 kg H_2/kg metal for high temperature metal hydrides [30]. Up-to-date studies have shown that metal hydrides allow the development of storage units that occupy 15 times less space in comparison to pressurized gaseous H_2 storage tanks (150 bar) while having the same weight. Additionally, metal hydrides can provide highly purified H_2 at their output resulting in the elongation of the fuel cell's lifetime and outmatch gaseous storage on safety, because absorption and desorption processes are taking place at nearly atmospheric conditions [35]. However, the most significant drawbacks of this storage method for application in decentralized power systems comprise the slow desorption and absorption rate of the storage tank, the need for additional amount of heat during the desorption process and the high costs that do not allow this method to compete gaseous storage, but only for capacities up to some tens of N m^3 [32].

Finally, underground reservoirs can be used for the storage of large H_2 amounts (up to 10^9 N m^3) at pressures of ~40 bar. Physical aquifers or salt caverns are most commonly used, but cannot be utilized for decentralized power systems due to high investment costs [47,48].

Fuel cells, hydrogen ICEs and hydrogen gas turbines can be used as the energy production unit of an energy-hydrogen storage hybrid power generation plant. Fuel cells comprise the most promising electricity production technology, due to their high efficiency at partial and full load, low emissions, fuel flexibility, and quiet operation. However, fuel cells have to confront competition from conventional gas turbines with similar efficiency and investment costs of 600–800 €/kW. Thus, fuel cells are expected to be initially integrated at systems with nominal power between 30 kW and 10 MW, since they cannot compete conventional gas turbines for higher power output due to financial reasons [32]. Alkaline electrolyte and PEM fuel cells of a few hundreds of kW are most appropriately applied in stand-alone power systems due to their short start-up times and the consumption of highly purified oxygen. Molten carbonate and solid oxide fuel cells can also be used, but are not in the scope of this article due to the use of natural gas or other hydrocarbons. PEM fuel cells have low operating temperatures (about 80 °C) leading to short start-up times and less corrosion of their components. However, their lifetime should reach 40,000 h of operation and the capital cost should initially drop down to 1000 $/kW and thereafter to 400–750 $/kW in order to become commercially competitive. On the other hand, the low cost and high efficiency of alkaline fuel cells outweigh the high sensitivity of their electrolyte to carbon dioxide and the shortening of their lifetime, and makes them the most attractive candidate for application in a decentralized energy-hydrogen storage hybrid power generation plant. Specifically, the fact that the production and consumption of hydrogen are taking place in the same location along with the important advantages of this type of cells can bring them back to the forefront [49–52]. Hydrogen ICEs are characterized by lower efficiency, but longer lifetime and lower costs compared to fuel cells. However, Vandenborre Hydrogen Systems introduced combined heat and power systems with nominal power ranging between 30 and 130 kW, which can reach an electrical efficiency of 35% and a total of 90%. Partial load operation can cause a decrease of the electrical efficiency significantly below 35%, which leads to the conclusion that hydrogen ICEs are more appropriate for applications where base load is largely constant and large amounts of heat are needed for the satisfaction of thermal loads. Finally, the use of hydrogen gas turbines requires some modifications in the design of conventional gas turbines. The very clean combustion that can be achieved with hydrogen results to the avoidance of blades corrosion phenomena and in the application of significantly higher turbine inlet temperatures. The very clean H_2 combustion prevents blade corrosion phenomena from occuring and allows for significantly higher turbine inlet temperatures and efficiencies compared to conventional gas turbines [32].

5. Simulation of a micro-CAES system using IPSE-pro software

5.1. Systems and main assumptions

The present paper evaluates the energetic and exergetic performance of four micro-CAES systems. Single- and two-stage systems

without air preheating before the turbine inlet will be studied and the effect of air preheating by waste heat recovery and fuel combustion on the system performance will then be investigated. Figs. 5–8 present the four examined systems as first presented by Kim and Favrat [26].

In order to study the performance of the systems and highlight their specific characteristics, the following assumptions were adopted:

- Steady state analysis with an air flow rate of 1.2 kg/s and compression up to 40 bar.
- Constant pressure in the storage tank.
- Isentropic efficiencies of the compressor and the turbine are equal to 0.85 and 0.87 respectively.
- For the two-stage systems the pressure ratios of both compressors and turbines are equal to each other with an intermediate pressure of 6.3 bar.
- Compressed air is preheated in the heat recuperator and the combustion chamber operating with natural gas.
- λ was assumed to be equal to 3.8 kg/kg in the single-stage and 3.6 kg/kg in the two-stage system.

5.2. Energetic analysis

The efficiency of the CAES systems will be evaluated in terms of energy storage and utilization of the compression and expansion waste heat. The electric storage efficiency is defined as:

$$\eta_{el.st.} = \frac{\sum_{i=1}^{j} P_{T_i} - \sum_{i=1}^{j} Q_{f_i} \eta_P}{\sum_{i=1}^{j} P_{C_i} + \sum_{i=1}^{k} P_{P_i}}, \quad (1)$$

where P_T is the power output of the j turbines, $Q_f\ \eta_p$ the energy produced in the j combustion chambers, with η_P being the efficiency of a conventional power plant for base-load charging, while P_C and P_P are the power inputs to the j compressors and k water pumps used for the water-cooled heat exchangers, respectively. The numerator of eq. (1) represents the opportunity cost of operating the CAES plant, i.e. the energy loss from burning the fuel in the CAES plant instead of using it for energy production in a conventional power plant.

The heating and cooling efficiencies are described by:

$$\text{heating efficiency}: \eta_{heating} = \frac{\sum_{i=1}^{j} Q_{aC_i}}{\sum_{i=1}^{j} P_{C_i} + \sum_{i=1}^{k} P_{P_i}}, \quad (2)$$

$$\text{cooling efficiency}: \eta_{cooling} = \frac{\sum_{i=1}^{j} Q_{ae_i}}{\sum_{i=1}^{j} P_{C_i} + \sum_{i=1}^{k} P_{P_i}}, \quad (3)$$

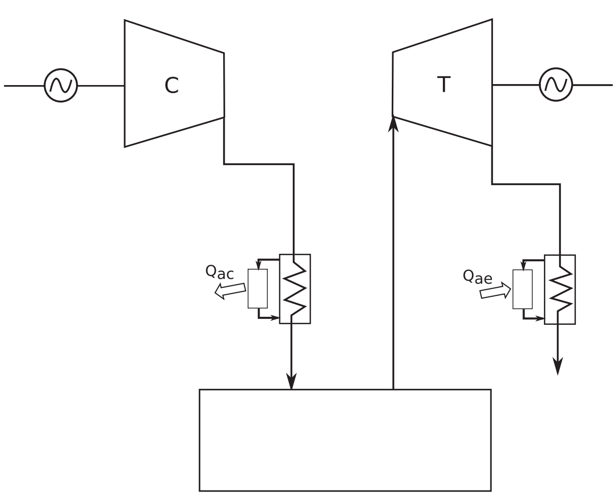


Fig. 5. Single-stage micro-CAES system without air preheating [16].

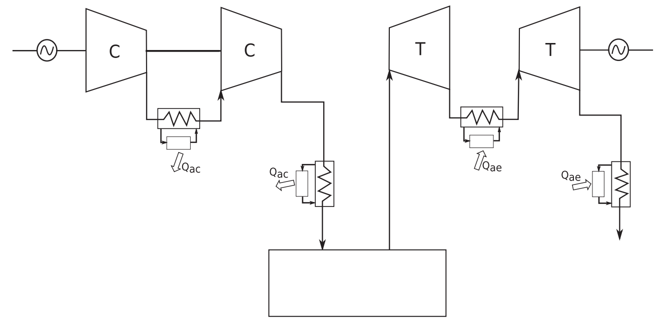


Fig. 6. Two-stage micro-CAES system without air preheating [16].

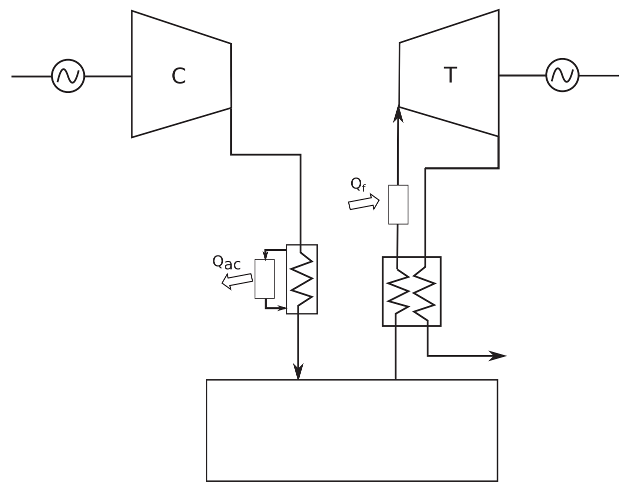


Fig. 7. Single-stage micro-CAES system with air preheating [16].

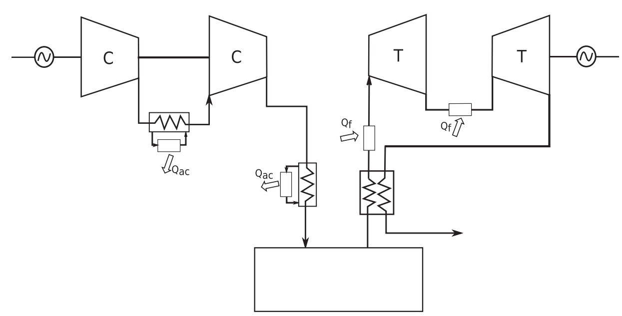


Fig. 8. Two-stage micro-CAES system with air preheating [16].

where Q_{ac} and Q_{ae} are the dissipated heat after compression and heat extracted after expansion, respectively.

Finally, the thermal efficiency of the plant will be defined only for systems with air preheating in order to provide an overview of the operation of the plant and a comparison measure to conventional gas turbine power plants. However, it is worth mentioning that the operational principles of these plants differ significantly from each other. Thus, thermal efficiency is only an artificial efficiency for CAES systems and will be defined as:

$$\eta_{th} = \frac{\sum_{i=1}^{j} P_{T_i} - \left(\sum_{i=1}^{j} P_{C_i} + \sum_{i=1}^{j} P_{P_i}\right)}{\sum_{i=1}^{j} Q_{f_i}}, \quad (4)$$

where Q_{f_i} represents the LHV of the fuel.

5.3. Exergetic analysis

Concerning the exergetic analysis of the storage plant, only the physical and chemical components of exergy will be considered in the calculation process, i.e. the dynamic and kinetic components will be neglected. Note that chemical exergy does not imply any chemical reaction, but the thermodynamic distance between the system and its surroundings.

The physical exergy component of the air and water flows through the heat exchangers is calculated by:

$$\dot{E}^{PH} = \dot{m}[h-h_0-T_0(s-s_0)] \tag{5}$$

where the zero index stands for the reference state ($p_0=1$ atm and $T_0=298.15$ K). The chemical exergy component is equal to zero for the air stream due to the similarity of its chemical composition to the system surroundings, while the exergy of the water stream is given by:

$$\dot{E}^{CH} = \dot{m}\frac{\overline{e}^{CH}}{M} \tag{6}$$

where M stands for the molar mass of water and $\overline{e_w}^{CH}=45$ kJ/kmol is the specific chemical exergy of water (model I) or $\overline{e_w}^{CH}=900$ kJ/kmol (model II) as both of the models are defined in [53].

The exergy destruction for each system component is calculated by:

$$\dot{E}_D = \sum_j \left(1-\frac{T_o}{T_j}\right)Q_j - W_{cv} + \sum_i \dot{m}_i e_i - \sum_e \dot{m}_e e_e \tag{7}$$

where $\dot{E}_D$ represents the exergy destruction, $\dot{E}_i = \sum_i \dot{m}_i e_i$ and $\dot{E}_e = \sum_e \dot{m}_e e_e$ stand for the rates of exergy transfer into and out of the control volume, W_{cv} is the energy transfer rate by work and $\sum_j(1-(T_o/T_j))Q_j$ the exergy transfer rate by heat. The first term of the equation was neglected in the present study due to the selection of the control volume of each system component in a way that the heat transfer takes place at 25 °C. The overall exergetic efficiency of the systems was calculated as follows:

$$\eta_{\Pi_{CAES}} = \frac{\sum_{i=1}^{j} Q_{ae_i} + \sum_{i=1}^{k} \Delta\dot{E}_{i,heatex.} + \sum_{i=1}^{l} \Delta\dot{E}_{i,fuelpreh.}}{\sum_{i=1}^{j} P_{C_i} + \sum_{i=1}^{k} P_{P_i} + \sum_{i=1}^{m} \dot{E}_{i,\,fuel}} \tag{8}$$

where $\Delta\dot{E}_{i,heatex.}$ and $\Delta\dot{E}_{i,fuelpreh.}$ stand for the exergy change of the streams flowing through the heat exchanger and the fuel preheater respectively and $\dot{E}_{i,fuel}$ represents the exergy of the incoming fuel stream.

5.4. Results and discussion

The exergy destruction for the CAES systems without and with air preheating is provided in Tables 2 and 3, respectively. In the single-stage system without air preheating more than 50 % of the exergy destruction takes place in the heat exchanger. This was expected as the flow entering the heat exchanger ($h_{in}=657.02$ kJ/kg, $T_{in}=624.09$ °C) is converted to a low energy quality flow ($h_{out}=20.1$ kJ/kg, $T_{out}=20$ °C).

Comparing the single to the two-stage system, the total exergy destruction of the multistage is 111.99 kW less than the single-stage system due to the lower destruction in the heat exchangers (in total, 79.3 kW less than the single-stage system). The increase in the exergy destruction of the compressors is balanced by the decrease in the destruction of the turbines, while approximately the same amount of exergy is destroyed in the pumps and the storage tank.

Comparing the single-stage systems with and without air preheating, the total exergy destruction for the former is higher by 257.44 kW as the decrease in the exergy destruction due to the replacement of the heat exchanger at the turbine outlet by a heat recuperator for air preheating is offset by the high exergy destruction in the combustion chamber. For the single-stage system with air preheating approximately 78% of the total exergy destruction is attributed to the combustion chamber and the heat exchanger at the compressor outlet.

For two-stage systems, the significant increase in the exergy destruction (572.02 kW) for the one with air preheating can be also attributed mainly to the fuel combustion before the HP and LP turbines, where ~55% of the total destruction occurs.

The efficiency values for the investigated CAES systems is listed in Table 4. For the systems without air preheating, the increased storage efficiency of the two-stage system (9.83 % higher compared to that of the single-stage) reveals the significant effects of intercooling and reheating. Storage efficiency increases considerably for systems with air preheating since fuel combustion before the expansion in the HP and LP stages leads to increased power outputs from the turbines. In contrast to the systems without preheating, the addition of a second compression and expansion stage does not contribute to higher storage efficiency.

As for the heating efficiency, it slightly differs among the various systems because of the very similar structure of the systems up to the storage tank and the low work input into the additional pumps. The cooling efficiency can only be defined for the systems without air preheating, as the low-temperature air streams after the turbine outlet can be used for the satisfaction of cooling needs. The employment of a second expansion stage

Table 2
Exergy destruction term for the various system components of the single- and two-stage systems without compressed air preheating.

Component	Single-stage system	Two-stage system	Single-stage system	Two-stage system
	$\dot{E}_D$ (kW)	$\dot{E}_D$ (kW)	Percentage of total $\dot{E}_D$	
LP compressor	47.76	27.88	8.77	6.44
LP water pump	1.33	0.46	0.24	0.11
LP heat exchanger	292.92	56.99	53.77	13.17
HP compressor	–	29.61	–	6.84
HP water pump	–	1.16	–	0.27
HP heat exchanger	–	157.63	–	36.42
Storage tank	0.54	0.54	0.1	0.13
HP turbine	–	23.96	–	5.54
HP water pump	–	0.19	–	0.04
HP heat exchanger	–	41.69	–	9.63
LP turbine	70.99	30.87	13.03	7.13
LP water pump	0.43	0.21	0.08	0.05
LP heat exchanger	130.76	61.55	24.01	14.23
Total	**544.73**	**432.74**	**100.00**	**100.00**

Table 3
Exergy destruction term for the various system components of the single- and two-stage systems with compressed air preheating.

Component	Single-stage system	Two-stage system	Single-stage system	Two-stage system
	$\dot{E}_D$ (kW)	$\dot{E}_D$ (kW)	Percentage of total $\dot{E}_D$	
LP compressor	45.76	27.88	5.94	2.77
LP water pump	1.33	0.46	0.17	0.05
LP heat exchanger	292.92	56.99	36.43	5.67
HP compressor	–	29.61	–	2.95
HP water pump	–	1.16	–	0.11
HP heat exchanger	–	157.63	–	15.69
Storage tank	0.54	0.54	0.06	0.05
Recuperator	43.53	110.15	5.41	10.96
Choke valve	6.29	6.29	0.78	0.63
1st combustion chamber	–	334.77	–	33.32
HP turbine	–	35.43	–	3.53
2nd combustion chamber	334.77	212.38	41.63	21.14
LP turbine	77.03	31.47	9.58	3.13
Total	**802.17**	**1004.76**	**100.00**	**100.00**

Table 4
Various efficiencies of the four micro-CAES systems.

	Single-stage without air preheating (%)	Two-stage without air preheating (%)	Single-stage with air preheating (%)	Two-stage with air preheating (%)
Electrical storage efficiency, $\eta_{el.st.}$	24.79	34.62	62.09	61.18
Heating efficiency, $\eta_{heating}$	98.3	98.09	98.48	98.28
Cooling efficiency, $\eta_{cooling}$	30.15	34.49	–	–
Thermal efficiency, η_{th}	–	–	7.98	23.82
Overall exergetic efficiency, $\eta_{\Pi_{CAES}}$	34.54	41.44	58.49	51.01

contributes to the increase of the cooling efficiency by 4.34 %. For the systems with air preheating, the reheating of the working medium before its expansion in the LP turbine results in an increase of the thermal efficiency by 15.84%.

From the exergetic point of view, the introduction of second compression and expansion stages increases the exergetic efficiency for the systems without air preheating. This can be attributed to the increase in the total work produced and the total heat extraction after the turbines. For systems with air preheating, a second stage causes an important drop in the exergy efficiency of the system. The additional work produced by expanding the reheated stream in the LP turbine is not enough to compensate for the chemical energy added in the LP combustion chamber. Comparing systems without and with air preheating, the higher exergy efficiency of the latter is attributed to the increased power output from the turbines which offsets the decrease due to the inability to use the expanded medium for cooling.

6. Simulation of an energy–hydrogen storage hybrid power generation system

In the present part of the study, a hybrid power generation system with wind turbines and hydrogen storage has been simulated and applied to a settlement of the Greek island of Karpathos. The load of the settlement was assumed to correspond to 5% of the total energy consumption of the island [54].

6.1. Input data

Based on the hourly averaged load data provided by the Public Power Corporation S.A. [55] for the island (2009), the load fluctuation map and the scaled monthly averaged data are shown Figs. 9 and 10, respectively.

The annual averaged load of the island is 207 kW with an energy consumption of 4.98 MWh/day, while the electrical load is nearly doubled in the summer months reaching 403 kW. This is attributed to the abrupt increase of the residents of the island during the high season and the increased cooling loads. Wind data [56] are obtained by wind measurements at a height of 40 m. With a Weibull shape factor of 1.6 and under the assumption that the wind speed peaks at 3 p.m. the scaled monthly averaged wind data and the corresponding Weibull distribution are provided in Figs. 11 and 12, respectively.

6.2. Input variables

6.2.1. Wind turbines

Two parameters need to be specified for the selection of the wind turbines: the nominal power and the number of turbines to be installed. Based on the peak load of the settlement, the wind energy integration in the urban environment and the wind farm operation during maintenance and failure periods, the Fuhrländer 100 turbines (P_{nom} = 100 kW) have been selected from the range of wind products that are provided from the software. Wind farms with nominal power ranging between 700 kW and 1000 kW were investigated.

6.2.2. Electrolyzing unit

For the electrolyzing unit, the optimal nominal power has been selected in the range 400–900 kW, while a typical efficiency value of 84% was assumed. The selection of the nominal power range

aims at the optimal utilization of the excess electricity produced by the wind farm.

6.2.3. Hydrogen storage tank

Hydrogen was stored in gaseous form in tanks with capacities between 750 and 1000 kg H_2. The capacity range was selected to take into account the current level of technology and to enable meeting the demand at time periods with insufficient wind energy production. The storage tank was initially filled to 95% of its total capacity.

6.2.4. Fuel cell

The nominal power range of the fuel cell has been specified between 450 and 600 kW in order to be able to satisfy the peak demand. A representative value of 44% has been selected for the electrical efficiency of the cell, while it has been assumed to have a lifetime of 40,000 operating hours.

6.2.5. System requirements

Meeting the electricity demand of the settlement without interruptions and fossil fuel independence are the basic requirements of the stand-alone power system. The intermittent operation of the system over its lifetime is ensured by requiring the year-end storage tank level to equal or exceed the initial tank level. The storage tank level should not reach zero even at peak demand and no wind energy production, while the fuel cell nominal power should exceed the peak load.

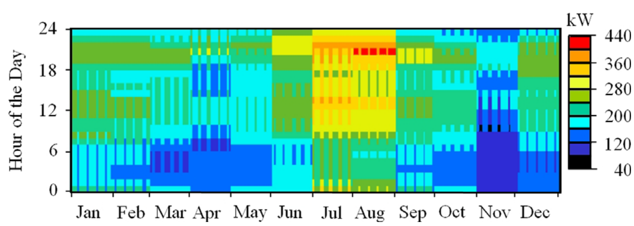


Fig. 9. Hourly load fluctuation map for 2009.

6.3. Results and discussion

With the use of the HOMER Energy software, the operation of 576 diverse plants was simulated to find the optimal operating system. The optimal plant consists of:

- 9 Fuhrländer 100 wind turbines with a nominal power of 100 kW and hub height of 35 m.
- A 700 kW electrolyzing unit with an efficiency of 84%.
- A hydrogen storage tank with a capacity of 1000 kg H_2, initially filled to 95% of its capacity.
- A 450 kW PEM fuel cell with an electrical efficiency of 44% and a lifetime of 40,000 operating hours.

Based on the wind speed and load data input and the optimization results, the time fluctuation of the wind power production and of the electrolyzer power input are provided in Figs. 13 and 14 respectively.

The mean wind power output is equal to 520 kW with a capacity factor of 57.8%, while an annual production of 4,554,623 kWh was obtained.

In Fig. 14 the expected proportional relation between the wind energy output and the electrolyzer power input can be partly distinguished. However, despite the simultaneous increase in the

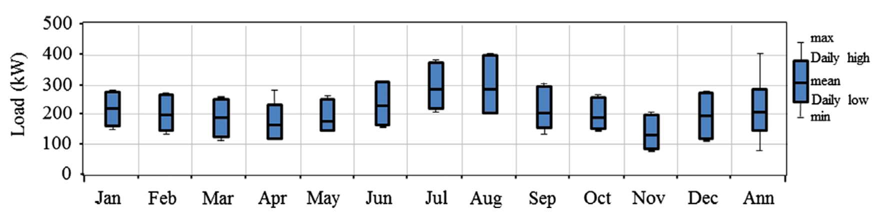


Fig. 10. Scaled monthly and annual averaged load data for 2009.

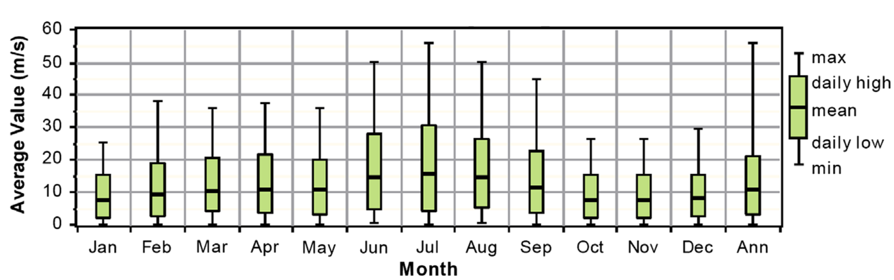


Fig. 11. Scaled monthly and annual averaged wind data for 2009.

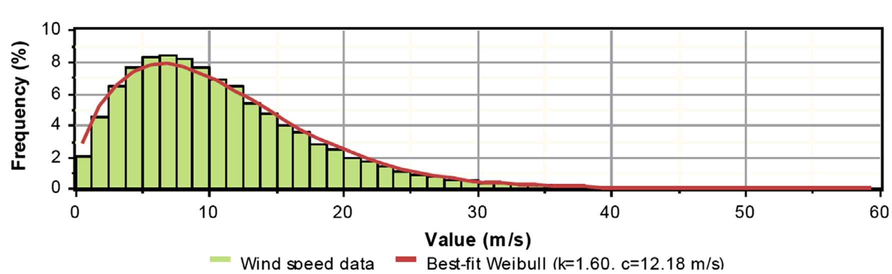


Fig. 12. Weibull distribution corresponding to the wind speed data for 2009.

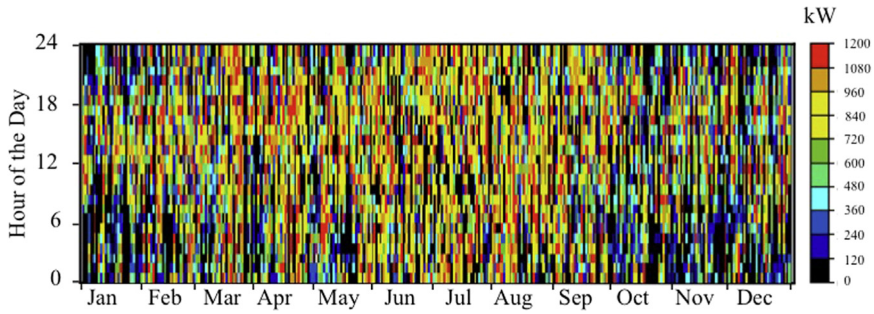


Fig. 13. Time fluctuation map of the wind power production.

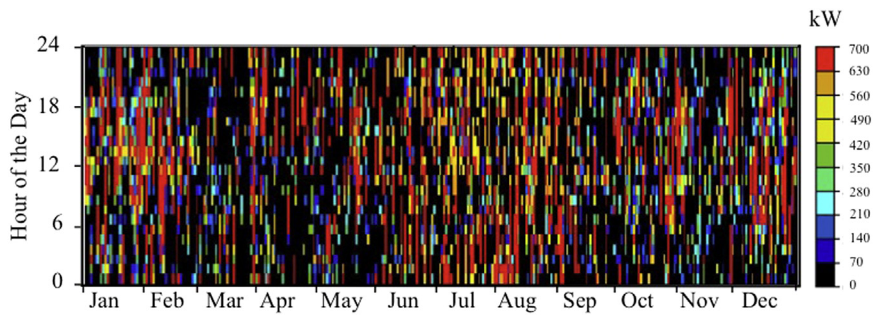


Fig. 14. Time fluctuation map of the electrolyzer power input.

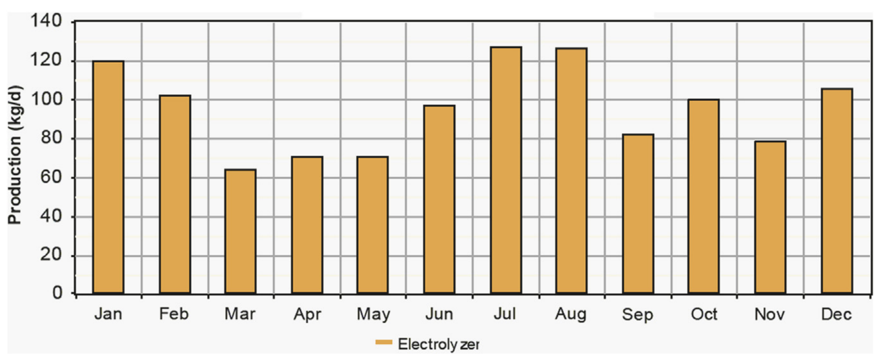


Fig. 15. Monthly averaged hydrogen production of the electrolyzing unit.

wind speed and slight decrease of the electrical load between February and May there is no distinguishable increase in the electrolyzer power input. This can be attributed to the high H_2 level in the storage tank as shown in Fig. 16, which does not allow the operation of electrolyzer at its nominal power. Excess electricity can be used to satisfy the electrical load in the rest of the island. During summer months, the high electrical load is mostly met by the increased wind energy production and the excess electricity is used for the production of H_2 only at times when the H_2 tank storage level allows it. In the end of October and until the first days of November the electrolyzer power input decreases considerably due to the reduced wind power production. Specifically, stored H_2 is used to meet the demand in the end of October and the storage tank reaches its lowest level of 186 kg H_2 on the 25th of that month. During the first days of November, the important decrease in the electricity demand results in high excess electricity despite the low wind power production. The electrolyzer operates close to its nominal power and the tank is filled up to its full capacity. As a result, the electrolyzer can not operate until the 23th of November and the excess electricity from the wind farm is rejected. During the last week of November, the electrolyzer power input is close to the nominal power and decreases in the first three weeks of December due to the very high tank storage level and the low excess electricity. Finally, the power input increases during the last week of the year due to the high wind power and the tank is filled up to its capacity.

The mean electrolyzer power input is 186.3 kW with a capacity factor of 26.6%, while a total annual consumption of 1,632,273 kWh/yr and a specific consumption of 47 kWh/kg H_2 were obtained. The electrolyzer operates 3398 h/yr, the mean and the maximum output are equal to 3.97 kg H_2/h and 14.91 kg H_2/h respectively and 34,760 kg H_2 are produced annually. Fig. 15 shows the monthly averaged H_2 production. The highest H_2 production was obtained during the months with increased wind energy production (July and August), which is adequate to offset the simultaneous increase in the electrical load during high season.

The time fluctuation map of the hydrogen tank storage level is shown in Fig. 16. The energy storage capacity of the tank and its autonomy are equal to 33,333.4 kWh and 161 h respectively, while the year-end tank level is 995 kg H_2 and exceeds the initial tank level (950 kg H_2).

Based on the input data and the operating behavior of the other components of the system, the fuel cell power output is presented in Fig. 17. The fuel cell operates close to its nominal power at peak demand times (July and August) and produces a low output mainly during November due to the low electricity demand.

The mean fuel cell power output is 151 kW with a capacity factor of 14.2% and specific hydrogen consumption of 0.071 kg

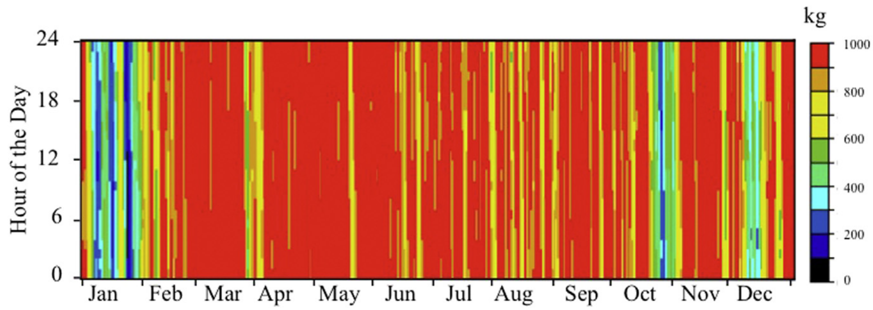


Fig. 16. Time fluctuation map of the hydrogen tank storage level.

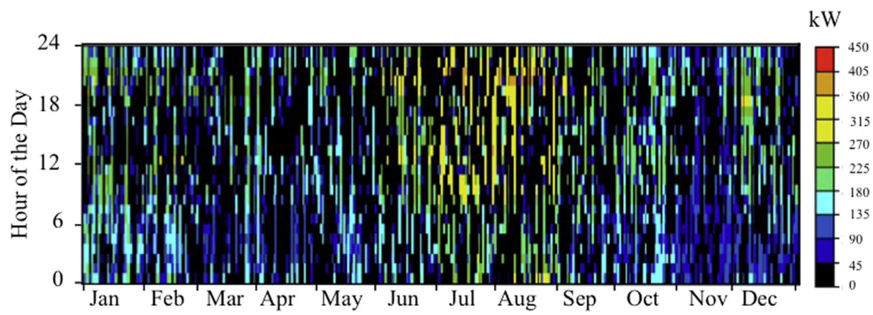


Fig. 17. Time fluctuation map of the fuel cell power output.

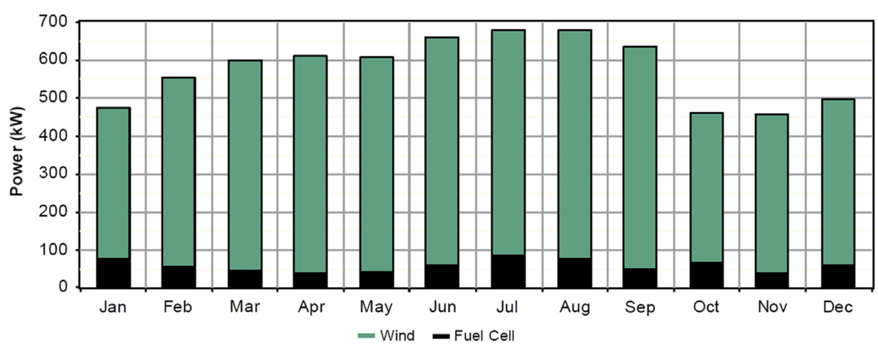


Fig. 18. Total monthly averaged electric power production of the wind farm and the fuel cell.

H_2/kWh. The fuel cell operates 3233 h/yr, consumes 34,716 kg H_2/yr and produces 489,323 kWh/yr. The mean electrical efficiency of the cell is equal to 42.3% and the cell starts 806 times/yr.

The total monthly averaged electric power production of the wind farm and the fuel cell are presented in Fig. 18. The total electric energy production is equal to 5,043,945 kWh/yr and 90% of this amount is produced by the wind turbines. The electric demand is fully met through the year, but the very high hydrogen tank storage level results in the rejection of 1,595,047 kWh/yr of excess electricity. However, this amount can be used as an input to another electrolyzing unit for the production of hydrogen and its use in the transportation sector. Alternatively, it can be utilized for the satisfaction of the electric demand in other settlements of the island.

7. Dynamic analysis of the compressed air energy storage system and comparison to the hybrid energy–hydrogen storage power generation system

7.1. Dynamic analysis of the CAES system

In this section, the two-stage compressed air energy storage system without air preheating will be dynamically examined. This system is selected due to its higher energetic and exergetic efficiency compared to the single-stage system and its clean technology.

7.1.1. Input variables

The wind and load input data are considered to be the same as in the case of the hybrid energy–hydrogen storage power generation system. For comparison reasons, the same wind farm as in the previous section is studied. Thus, Fig. 8 presents the time fluctuation map of the wind power production also in the case of the CAES system.

7.1.2. Compressor unit

The technical characteristics of the compressors are as stated in Section 5.1 and their cumulative power sums up to the nominal power of the electrolyzing unit (700 kW) for comparison reasons. In specific, the LP and HP compressors have a nominal power of 300 kW and 400 kW respectively. Another important issue referring to the operational principles of the compressors is that their minimum load is set to 10%.

7.1.3. Compressed air storage tank

The storage capacity of the tank for the execution of the HOMER software was set to 1000 kg H_2 corresponding to 33,333.4 kWh of thermal energy and an autonomy of 161 h. In

order to assure that the compressed air storage tank will have the same capacity as the hydrogen tank, the energy density of the compressed air – given the enthalpy changes through the LP and HP turbines – should be calculated:

$$E = m\,\Delta h = 1\text{ kg}((20.1-(-83.59))\text{ kJ/kg} + (9.64-(-85.47))\text{ kJ/kg})$$
$$= 198.8\text{ kJ} = 0.0552\text{ kWh}$$

Thus, the compressed air storage tank capacity was set equal to 603,622.94 kg of compressed air and the tank was initially filled to 95% of its total capacity.

7.1.4. Expansion unit

The functional characteristics of the turbines are as stated in Section 5.1 and the cumulative power of the HP and LP turbines was set to 230 kW and 220 kW respectively, summing up to the nominal power of the fuel cell (450 kW). The isentropic and mechanical efficiency of the turbines are $\eta_{is,T}=0.87$ and $\eta_{m,T}=0.99$ respectively.

7.1.5. System requirements

As previously stated, the most important parameter to ensure the uninterruptible operation of the system is the year-end tank level to be equal or higher than the initial tank level. Furthermore, the storage tank should not reach zero level even under extreme conditions (peak demand and no wind energy production), while the total power of the turbines should exceed the peak load.

7.1.6. Results and discussion

Based on the wind power production and load data, excess electricity for every hour of the year will be used as the compressor power input:

$$P_{comp} = P_{el}\,\eta_{el,M}\,\eta_{m,M}\ (\text{kW}) \tag{9}$$

where P_{comp} the total power input to the compressors, P_{el} the excess electricity, and $\eta_{el,M}$, $\eta_{m,M}$ the electric and mechanical efficiency of the motors respectively. The total air mass flow rate through the compressors is given by:

$$\dot{m} = \frac{P_{comp}\,\eta_{m,comp}}{(\Delta h_1 + \Delta h_2)}\ (\text{kg/s}) \tag{10}$$

where $\eta_{m,comp}$ the mechanical efficiency of the compressors and Δh_1, Δh_2 the enthalpy change at the LP and HP compressors respectively.

Based on the hourly electricity deficit, the total power output and the air mass flow rate through the turbines is provided by:

$$P_{turb} = \frac{P_{el}}{\eta_{el,G}\,\eta_{m,G}}\ (\text{kW}) \tag{11}$$

$$\dot{m} = \frac{P_{turb}}{\eta_{m,turb}(\Delta h_1 + \Delta h_2)}\ (\text{kg/s}) \tag{12}$$

where P_{turb} the total power output, P_{el} the electricity deficit, $\eta_{el,G}$, $\eta_{m,G}$ the electric and mechanical efficiency of the generator, $\eta_{m,turb}$ the mechanical efficiency of the turbine and Δh_1, Δh_2 the enthalpy change at the HP and LP turbines respectively.

The level of the compressed air storage tank is calculated from the mass flows entering and leaving the tank. A disconnection of the compressors is foreseen at times when the tank is filled up to its full capacity.

Fig. 19 shows the total power input to the compressors as a function of the wind energy production. P_{comp} increases with increasing wind power generation as expected. For wind power production above 850 kW the compressors operate mostly close to their nominal power. Zero power input to the air compressors can occur over the whole range of wind power production due to the inability of the wind farm either to meet the demand or to deliver excess power above 70 kW, or due to the high storage tank level which results in rejecting excess electricity. The mean total power input was 160.23 kW with a capacity factor of 22.9%. The total annual electricity consumption and the specific consumption of compressed air are 1,403,574 kWh/yr and 0.1613 kWh/kg compressed air respectively. The mean production rate of compressed air is 1023.58 kg/h, while the maximum rate and the yearly production amount to 4473 kg/h and 8,966,595 kg/year respectively. Fig. 20 presents the monthly averaged compressed air production in kg/day.

Fig. 21 shows the total power output from the turbines as a function of the load. In general, an increase of the turbine power output can be observed with the increase of the load. In specific, the linear dependence of these two parameters is profound during the periods of zero wind power generation, when the total load is met by the electricity generated by the air turbines. The operating points between the x-axis and the identity line represent time periods when the load is met from both the wind

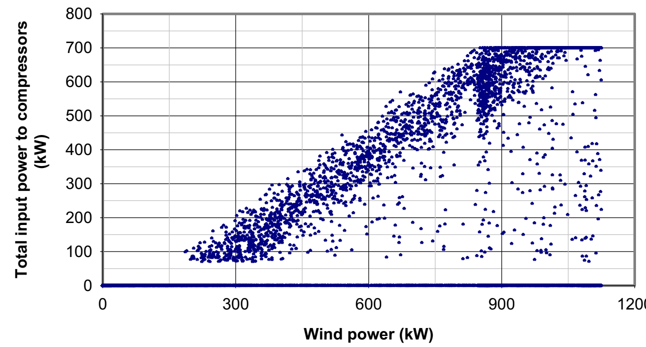


Fig. 19. Total input power to compressors as a function of wind power generation.

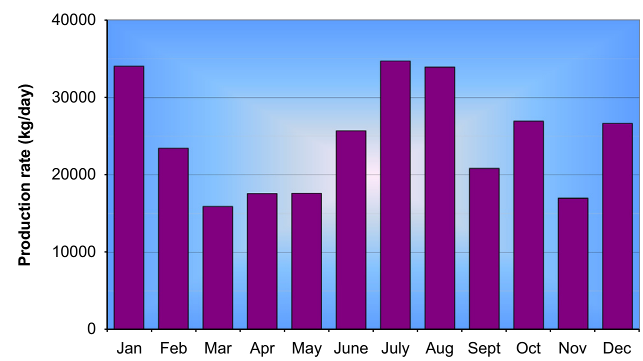


Fig. 20. Monthly averaged compressed air production.

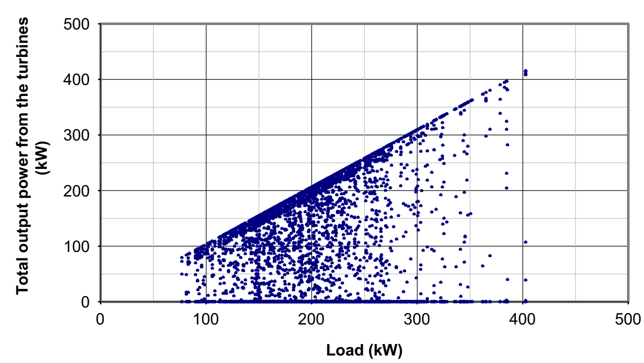


Fig. 21. Total output power from the turbines as a function of the load.

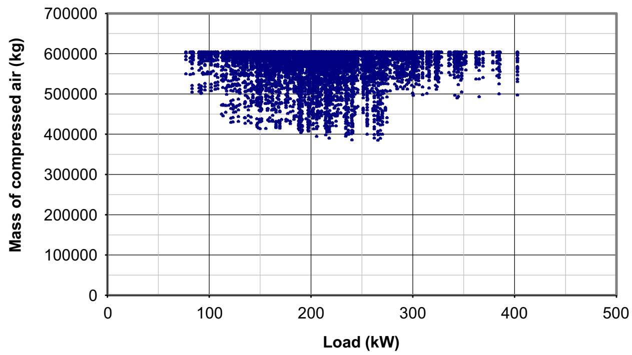


Fig. 22. Content of the storage tank as a function of the load.

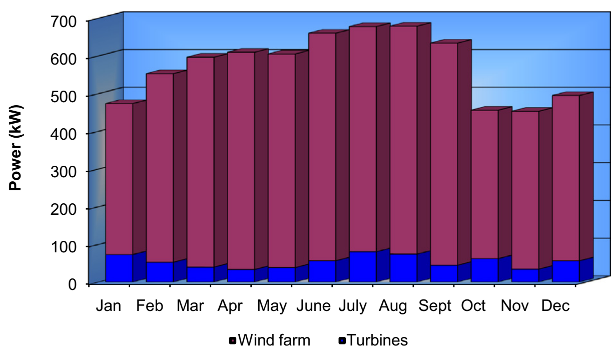


Fig. 23. Allocation of the monthly averaged electric production to the system components.

farm and the air turbines, while the points on the horizontal axis correspond to times when the load is fully met by the wind power generation. The mean total power output is equal to 55.78 kW with a capacity factor of 12.39% and an annual power production of 488,608 kWh. The turbines consume 8,937,414 kg air/year with a specific consumption of 18.85 kg air/kWh, while they operate 3023 h annually.

Based on the production of compressed air from the compressors and its consumption in the turbines, the content of the storage tank is provided in Fig. 22 as a function of the load. The minimum amount of air in the tank over the year is 384,811 kg which raises questions about oversizing of the storage tank.

Fig. 23 shows the total monthly averaged electric production of the wind farm and the turbines. The total annual electric production is equal to 5,043,226 kWh/yr with 90.3% of this amount produced by the wind farm and the remaining 9.7% by the turbines. The system is capable of fully meeting the electric demand through the year, but results in a considerable electricity excess (1,669,579 kWh/year). This excess amounts to 33.1% of the total electricity generation and can be used as an input to another electrolyzing unit for the production of hydrogen and its use in the transportation sector.

Finally, it is worth mentioning that the required power input to the water pumps involved in the CAES system was not accounted for. However, the energy consumption of the water pumps is negligible compared to the total electricity generation.

7.2. Comparison of the compressed air energy storage system to the hybrid energy–hydrogen storage power generation system

In this section, the hydrogen storage system and the two most efficient compressed air energy storage systems (two-stage without air preheating and single stage with air preheating) will be compared with respect to their efficiency and costs.

7.2.1. Efficiency

For the H_2 storage system, the electrolyzer and the fuel cell specific consumptions were calculated at 47 kWh/kg H_2 and 0.071 kg H_2/kWh respectively. Examining the system as a "black box" and assuming that the fuel cell consumes the exact amount of hydrogen produced by the electrolyzing unit, the energy storage efficiency can be calculated. Thus, assuming an electricity excess of 500 kWh during an hour of the year, the following is derived:

- amount of H_2 produced:

$$m = \frac{E}{f_{elect.}} = \frac{500\ \text{kWh}}{47\ (\text{kWh/kg})} = 10.64\ \text{kg}\ H_2$$

- energy output from the fuel cell:

$$E_{f.c.} = \frac{m}{f_{f.c.}} = \frac{10.64\ \text{kg}}{0.071\ (\text{kg/kWh})} = 149.83\ \text{kWh}$$

- energy storage efficiency:

$$n_{H_2} = \frac{E_{f.c.}}{E} = \frac{149.83\ \text{kWh}}{500\ \text{kWh}} = 0.2997 = 29.97\%$$

Fig. 24 presents the energy flow for the hydrogen energy storage system.

For the two-stage compressed air energy storage system, the specific energy consumption of the compressors and the turbines is 0.1613 kWh/kg air and 18.85 kg air/kWh respectively. Under the assumptions made for the hydrogen storage system and taking into account the power input to the water pumps, the energy storage efficiency will be calculated for an electricity excess of 500 kWh.

- amount of compressed air produced:

$$m = \frac{E}{f_{elect.}} = \frac{500\ \text{kWh}}{0.1613\ (\text{kWh/kg})} = 3100.2\ \text{kg air}$$

- total energy output from the HP and LP turbines:

$$E_{turb.} = \frac{m}{f_{turb.}} = \frac{3100.2\ \text{kg}}{18.85\ (\text{kg/kWh})} = 164.44\ \text{kWh}$$

- energy storage efficiency:

$$n = \frac{E_{turb.}}{E + E_{pump}} = \frac{149.83\ \text{kWh}}{(500 + 6.475)\ \text{kWh}} = 0.3247 = 32.47\%$$

Fig. 25 presents the energy flow for the two-stage compressed air energy storage system.

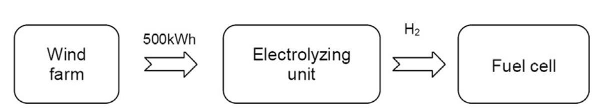


Fig. 24. Flow diagram for the hydrogen energy storage system.

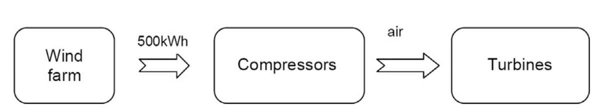


Fig. 25. Flow diagram for the two-stage compressed air energy storage system without air preheating.

Finally, the single-stage CAES system with air preheating will be examined. The operational characteristics of the system are provided in the following:

- amount of compressed air produced:

$$P_{comp} = P_{el}\,\eta_{el,M}\,\eta_{m,M}\ (\text{kW}) \tag{13}$$

$$\dot{m} = \frac{P_{comp}\,\eta_{m,comp}}{\Delta h}\ (\text{kg/s}) \tag{14}$$

- consumed amount of compressed air:

$$P_{turb} = \frac{P_{el}}{n_{el,G}\eta_{m,G}}\ (\text{kW}) \tag{15}$$

$$\dot{m} = \frac{P_{turb}}{\eta_{m,turb}\,\Delta h}\ (\text{kg/s}) \tag{16}$$

Examining the system as a "black box" and under the same assumptions as for the two previous systems, the energy storage efficiency was calculated. Fig. 26 presents the energy flow of the the single-stage compressed air energy storage system.

- air mass flow rate:

$$\dot{m} = \frac{P_{el}\,\eta_{el,M}\,\eta_{m,M}\,\eta_{m,comp}}{\Delta h_{comp.}} = \frac{500 \times 0.99 \times 0.99 \times 0.98\ \text{kW}}{(657.02-20.1)\ (\text{kJ/kg})}$$
$$= 0.75\ \text{kg/s} = 2.714\ \text{kg/h}$$

- energy output from the generators:

$$P_{el} = \dot{m}\,\Delta h_{turb.}\,\eta_{el,G}\,\eta_{m,G}\,\eta_{m,turb}\ (\text{kW}) \tag{17}$$

$$P_{el.} = 0.75\ \text{kg/s}\ (1055.4-351.78)\ \text{kJ/kg} \times 0.98 \times 0.99$$
$$\times 0.99 = 509.58\ \text{kW}$$

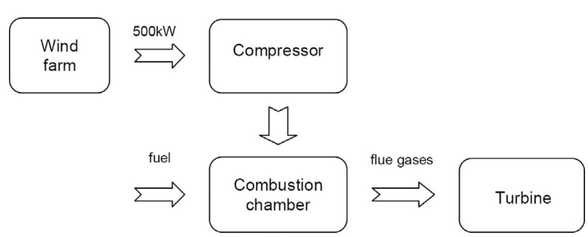


Fig. 26. Flow diagram for the single-stage compressed air energy storage system with air preheating.

with the enthalpy changes $\Delta h_{comp.}$ and $\Delta h_{turb.}$ as they were calculated in Section 5.

- energy storage efficiency:

$$n = \frac{P_T - Q\eta_P}{P_C + P_{pump}} = \frac{(509.58-47,897 \times 0.01198 \times 0.4)\ \text{kW}}{(500 + 4.163)\ \text{kW}}$$
$$= 0.5555 = 55.55\%$$

where Q represents the LHV of the fuel and η_P the thermal efficiency of a conventional power plant with 40% being a representative value.

It is worth mentioning that the difference in the energy storage efficiency values of the CAES systems as calculated in the present section compared to Section 5 can be attributed to the mechanical and electrical efficiencies of the motors and generators.

Table 5 summarizes the energy storage efficiency for the systems investigated. The two-stage CAES system is by 2.5% more efficient compared to the hydrogen energy storage system being the best option between the two CO_2-free technologies. The considerably higher efficiency of the single-stage CAES system with air preheating comes at a cost of CO_2 emissions and higher investment and O&M costs.

7.2.2. Costs

A cost summary and the net present cost were calculated for the H_2 system based on the cost data provided in Section 4. Table 6 represents the capital and operational costs of each system component.

For the calculation of the Net Present Cost, the annual real interest rate was taken equal to 6% with a project lifetime of 20 years. Since the lifetime of the wind farm and the fuel cell were set equal to 25 years and 40,000 h of operation respectively, the salvage value of these components was also accounted for. Fig. 27 shows the cash flow summary of the H_2 storage system and its allocation to the system components.

However, the presented cash flow summary contains important sources of uncertainty due to the fact that the system components are not technologically mature yet and that particular conditions need to be fulfilled for their efficient operation (high purity water needed as an input to the electrolyzer, low lifetime of PEM fuel cells should be improved, battery use required until the fuel cell reaches its operating temperature, decrease in the fuel cell efficiency over its lifetime).

Table 5
Energy storage efficiency for the energy storage systems investigated.

System	Hydrogen energy storage system (%)	Two-stage CAES system without air preheating (%)	Single-stage CAES system with air preheating (%)
Energy storage efficiency	29.97	32.47	55.55

Table 6
Capital and O&M costs for the hydrogen energy storage system.

System component	Capital cost(€)	Replacement cost (€)	O&M (€)	Salvage value (€)	Total (€)
Wind farm	2,550,000	0	585,000	−79,500	3,055,500
Fuel cell	1,350,000	656,500	85,200	−161,400	1,930,300
Electrolyzing unit	1,200,000	0	137,600	0	1,337,600
Storage tank	422,700	0	24,200	0	446,900
System	5,522,700	656,500	832,000	−240,900	6,770,300

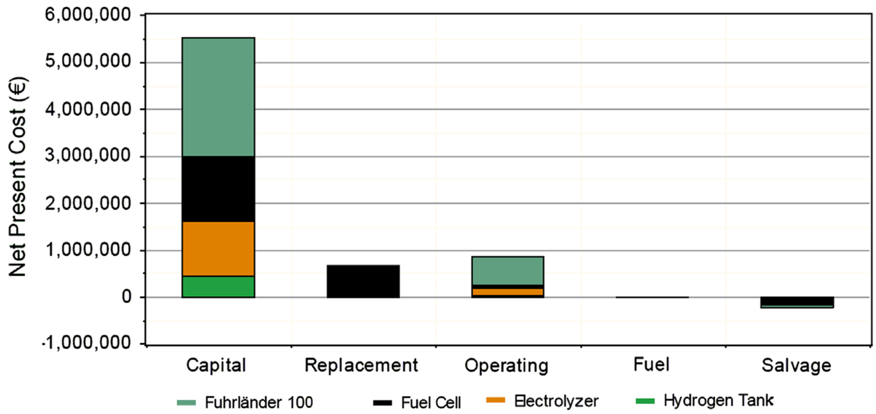


Fig. 27. Cash flow summary for the hydrogen energy storage system.

Table 7
Representative values of the capital cost of the CAES system.

System component	Compressors	Turbines	Generators	Storage tank	Wind farm	System
Capital cost (€)	1,820,000	1,170,000	1,170,000	1,330,000	2,550,000	8,040,000

Table 8
Advantages and drawbacks of the systems investigated.

	Energy-hydrogen storage system	Two-stage CAES without air preheating	Single-stage CAES with air preheating
Technology level	Immature	Mature	Mature
Capital costs	Need to lower the fuel cell capital costs to 400–750 €/kW. Capital costs of H_2 storage in metal hydrides need also to be lowered.	High cost due to the storage of air either in underground caverns or pipelines (infrastructure and civil engineering costs)	Lower than the two-stage system due to lower compressor nominal power and storage tank capacity
O&M costs	High due to the need of regular maintenance and well-educated technicians	High due to the maintenance of the moving parts.	Significantly higher due to the fuel costs. Higher uncertainty for the project due to the high volatility of natural gas prices.
Response time	Need to be reduced (battery use until fuel cells reach their operating temperature)	Relatively low	Relatively low
Efficiency	Significant decrease in the efficiency over the lifetime (fuel cell membrane, maintenance of the hydrogen compressor and the storage tank)	Approximately unchanged over lifetime (need for replacement of the air filters)	Approximately unchanged over lifetime (need for replacement of the air filters and cleaning of the flue-gas deposits)

Referring to the cost of the CAES system, approximate calculations were conducted due to lack of adequate cost data in order to specify the order of magnitude of the cost. In specific, the capital cost of the compressors, turbines and AC generators were taken equal to 2600 €/kW (given by the manufacturer of the T-CAES system) and the cost of the storage tank was assumed to be equal to 40 €/kWh as given by the manufacturer of the SCAES system. The capital cost of the wind farm was taken equal to 1500 €/kW and the interconnection cost was provided by:

$$\text{Interconnection Cost} = 300,000 + 100,000N \tag{18}$$

where N represents the number of the wind turbines. Table 7 provides the capital costs of the system and the allocation to its components.

By comparison of the H_2 and compressed air storage systems in terms of capital costs, it follows that the investment for a CAES system is considerably higher. The O&M costs were not calculated due to lack of sufficient data. However, it has to be considered that the system is composed of technologically mature components with many applications in the energy generation sector. On the other hand, the moving parts of the system as well as the fact that the system has to go out of service during the maintenance periods have a negative impact on the operating costs. As far as the single-stage CAES system with air preheating is concerned, there is a trade-off between the operating costs (fuel costs) and the lower capital costs. Specifically, the same amount of energy can be produced by the expansion of half the amount of compressed air that could have been used by a two-stage system without air preheating. That leads to the down-sizing of the compressor and the storage tank and decreases the capital costs of the system. Table 8 summarizes the advantages and drawbacks of the investigated systems.

8. Conclusions

The present study contained an energetic and exergetic analysis of four micro-CAES systems and investigated their operational behavior and efficiency. The single-stage system with air preheating and the two-stage without air preheating were proven to be more efficient from the energy and exergy point of view.

Referring to the hybrid energy–hydrogen storage power generation system, simulations were conducted using the HOMER Energy software and the system was applied to the island of Karpathos. Based on the input data and the system requirements and restrictions, the operational behavior of the system components and the electric power production of the wind farm and the fuel cell were investigated.

The dynamic analysis of the two-stage CAES system without air preheating contributed to the understanding of the performance of the system over the year. This was proven to be similar to the behavior of the H2 storage system.

The comparison of the two-stage CAES without preheating, the single-stage with air preheating and the hydrogen energy system with respect to their efficiency and financial viability suggested that the two-stage system is by 2.5% more efficient compared to the hydrogen storage system. As expected, the single-stage system was proven to be remarkably more efficient than the other two systems with negative effects on the O&M costs and the CO_2 emissions over the project′s lifetime.

Cost related data were presented to highlight the advantages and drawbacks of the systems. The capital costs of the CAES system make it less attractive compared to the hydrogen storage system. On the other hand, the O&M cost was expected to be higher for the hydrogen system as it is a power solution consisting of technologically immature components. However, the cost of the systems is a major parameter for its economic viability and a cost and sensitivity analysis should be conducted.

References

[1] Ibrahim H, Ilinca A, Perron J. Energy storage systems – characteristics and comparisons. Renewable and Sustainable Energy Reviews 2008;12(5):1221–50.
[2] Anzano JP, Jaud P, Madet D. Stockage de l' électricité dans le système de production électrique. Techniques de l'ingénieur, traité de Génie Électrique 1989;D4030.
[3] Haug R. The Iowa stored energy plant. DOE Energy Storage Systems Annual Peer Review ; 2006.
[4] Meyer F. Integration von regenerativen Stromerzeugern. Druckluft-Speicherkraftwerke, Projektinfo 05/2007.
[5] Nölke M. Compressed Air Energy Storage (CAES) – Eine sinnvolle Ergänzung zur Energieversorgung? Promotionsvortrag 2006.
[6] Zunft S. Diabate und adiabate Druckluftspeicherkraftwerke. 5.dena-Energie-Forum "Druckluftspeicherkraftwerke". Berlin 8 September 2005.
[7] Crotogino F. KBB Underground Technologies GmbH, Hannover, Compressed Air Storage, Internationale Konferenz "Energieautonomie durch Speicherung Erneuerbarer Energien", 30.–31. Oktober 2006.
[8] Oldenburg CM, Pan L. Porous Media Compressed-Air Energy Storage (PM-CAES): theory and simulation of the coupled wellbore-reservoir system. Transport in Porous Media 2013;97(2):201–21.
[9] Ibrahim H, Younès R, Ilinca A, Dimitrova M, Perron J. Study and design of a hybrid wind–diesel–compressed air energy storage system for remote areas. Applied Energy 2010;87(5):1749–62.
[10] Abbaspour M, Satkin M, Mohammadi-Ivatloo B, Hoseinzadeh Lotfi F, Noorollahi Y. Optimal operation scheduling of wind power integrated with compressed air energy storage (CAES). Renewable Energy 2013;53:53–9.
[11] Lund H, Salgi G, Elmegaard B, Andersen AN. Optimal operation strategies of compressed air energy storage (CAES) on electricity spot markets with fluctuating prices. Applied Thermal Engineering 2009;29(5–6):799–806.
[12] Salgi G, Lund H. System behaviour of compressed-air energy-storage in Denmark with a high penetration of renewable energy sources. Applied Energy 2008;85(4):182–9.
[13] Wang H, Wang L, Wang X, Yao E. A novel pumped hydro combined with compressed air energy storage system. Energies 2013;6(3):1554–67.
[14] Grazzini G, Milazzo A. A thermodynamic analysis of multistage adiabatic CAES. Proceedings of the IEEE 2012;100(2):461–72.
[15] Zhang Y, Yang K, Li X, Xu J. The thermodynamic effect of thermal energy storage on compressed air energy storage system. Renewable Energy 2013;50:227–35.
[16] Zhang Y, Yang K, Li X, Xu J. The thermodynamic effect of air storage chamber model on Advanced Adiabatic Compressed Air Energy Storage System. Renewable Energy 2013;57:469–78.
[17] Jakiel C. Entwicklung von Großdampfturbinen, Wärmespeichern und Hochtemperatur-Kompressoren für adiabate Druckluftspeicherkraftwerke. 5. dena-EnergieForum "Druckluftspeicherkraftwerke". Berlin 8. September 2005.
[18] Zunft S, Tamme R, Nowi A, Jakiel C. Adiabate Druckluftspeicherkraftwerke: Ein Element zur netzkonformen Integration von Windenergie. Energiewirtschaftliche Tagesfragen, 55. Jg. (2005), Heft 7.
[19] Nowi A, Jakiel C, Moser P Zunft S. Adiabate Druckluftspeicherkraftwerke zur netzverträglichen Windstrominegration. VDI-GET Fachtagung "Fortschrittliche Energiewandlung und -anwendung. Strom- und Wärmeerzeugung. Kommunale und industrielle Energieanwendungen", Leverkusen, 09.–10.Mai 2006.
[20] Nielsen L, Leithner R. Dynamic simulation of an innovative compressed air energy storage plant – detailed modelling of the storage cavern. World Scientific and Engineering Academy and Society (WSEAS) Transactions on Power Systems 2009;4(8).
[21] Institut für Transportation Design (ITD). Animation des GuD-Druckluftspeicherkraftwerks ISACOAST-CC ⟨http:/www.transportation-design.org/cms/front_content.php?idcatart=286⟩.
[22] Nielsen L, Qi D, Brinkmeier N, Leithner R. Isobares GuD-Druckluftspeicherkraftwerk mit Wärmespeicher (ISACOAST-CC) – Konzept und Simulationsergebnisse.
[23] Energie-Forschungszentrum Niedersachsen (efzn). Isobares GuD-Druckluftspeicherkraftwerk mit Wärmespeicher.
[24] Proczka JJ, Muralidharan K, Villela D, Simmons JH, Frantziskonis G. Guidelines for the pressure and efficient sizing of pressure vessels for compressed air energy storage. Energy Conversion and Management 2013;65:597–605.
[25] EA Techology. Review of electrical energy storage technologies and systems and of their potential for the UK; 2004.
[26] Kim YM, Favrat D. Energy and exergy analysis of a micro-compressed air energy storage and air cycle heating and cooling system. Energy 2010;35 (1):213–20.
[27] Li Y, Wang X, Li D, Ding Y. A trigeneration system based on compressed air and thermal energy storage. Applied Energy 2012;99:316–23.
[28] Ecofys GmbH. Verbesserte Integration großer Windstrommengen durch Zwischenspeicherung mittels CAES. November, 2006.
[29] Sigma-Aldrich Corporation. Hydrogen storage materials. Material Matters 2007;2(2).
[30] Sherif SA, Barbir F, Veziroglu TN. Wind Energy and the hydrogen economy – review of the technology. Solar Energy 2005;78:647–60.
[31] Lymberopoulos N, Varkaraki E, Zoulias M, Vionis P, Chaviaropoulos P, Agoris D. First steps in hydrogen production from wind energy in Greece; 2005.
[32] Zoulias M, Glöckner R, Lymberopoulos N, Vosseler I., Tsoutsos T, Mydske HJ, et al., Market potential analysis for the introduction of hydrogen energy technology in stand-alone power systems. HSAPS workshop; 2004.
[33] Gammon R, Roy A, Barton J, Little M. Hydrogen and renewables integration (HARI).UK: Centre for Renewable Energy Systems Technology (CREST), Loughborough University; 2006.
[34] Cicconardi SP, Jannelli E, Spazzafumo G. Hydrogen energy storage: preliminary analysis. International Journal of Hydrogen Energy 1993;18(11):933–40.
[35] Shanzbaatar A. Comparing hydrogen storage methods for efficient hydrogen power backup systems; 2007.
[36] U.S. Department of Energy – energy efficiency and renewable energy. Fuel cells technologies program – hydrogen storage, gaseous and liquid hydrogen storage.
[37] Züttel A. Materials for hydrogen storage. Materials Today 2003;6(9):24–33.
[38] Energy Systems Research Unit. University of Strathclyde, Glasgow, Hydrogen Storage.
[39] Zhou L. Progress and problems in hydrogen storage methods. Renewable and Sustainable Energy Reviews 2005;9(4):395–408.
[40] Liu B-H. Hydrogen–metal systems: hydride forming alloys (properties and characteristics, database information). Encyclopedia of materials: science and technology. Elsevier Science Ltd. 2001, p. 3953–69.
[41] Conte M, Prosini PP, Passerini S. Overview of energy/hydrogen storage: state-of-the-art of the technologies and prospects for nanomaterials. Materials Science and Engineering B 2004;108(1–2):2–8.
[42] Yang FS, Wang GX, Zhang ZX, Meng XY, Rudolph V. Design of the metal hydride reactors – a review on the key technical issues. International Journal of Hydrogen Energy 2010;35(8):3832–40.
[43] Veerraju Ch, Ram Gopal M. Heat and mass transfer studies on elliptical metal hydride tubes and tube banks. International Journal of Hydrogen Energy 2009;34(10):4340–50.
[44] Mohan G, Prakash Maiya M, Srinivasa Murthy S. Performance simulation of metal hydride hydrogen storage device with embedded filters and heat exchanger tubes. International Journal of Hydrogen Energy 2007;32 (18):4978–87.
[45] Dehouche Z, Peretti HA, Yoo Y, Belkacemi K, Goyette J. Catalyzed light hydride nanomaterials embedded in a micro-channels hydrogen storage container. Recent Patents on Nanotechnology 2009;3(2):116–34.
[46] Meng XY, Yang FS, Wang YQ, Deng JQ, Zhang ZX. Design and process simulation of a micro-channel chemical heat pump reactor. In: Proceedings of the Chinese chemical engineering machinery conference 2008; 2008.
[47] Institut für Kraftfahrzeuge (IKA). RWTH Aachen University. Large Hydrogen Underground Storage. ⟨http:/www.ika.rwth-Aachen.de/r2h/index.php/Large_Hydrogen_Underground_Storage⟩.
[48] Cleveland CJ. Fuel cells. The encyclopedia of earth; 2006.
[49] Hi-Energy. E4tech, element energy. Pure Energy Centre, Stationary and portable fuel cells information resource. Information Resource for Highlands & Islands Enterprise.
[50] U.S. Department of Energy – energy efficiency and renewable energy. Fuel cells technologies program – fuel cells. Types of fuel cells.
[51] National Fuel Cell Research Center, University of California, Irvine. Fuel cell types; 2009.
[52] International Partnership for the Hydrogen Economy (IPHE). Fuel cells: a hydrogen enabling technology.

[53] Bejan A, Tsatsaronis G, Moran M. Thermal design and optimization; 1996.
[54] NREL, "Homer: the optimization model for distributed power". 〈http:/www.homerenergy.com〉.
[55] Public Power Corporation S.A. 〈http:/www.dei.gr/Default.aspx?lang=2〉.
[56] Giatrakos GP, Tsoutsos TD, Mouchtaropoulos PG, Naxakis GD, Stavrakakis G. Sustainable energy planning based on a stand-alone hybrid renewable energy/hydrogen power system: application in Karpathos island, Greece. Renewable Energy 2009;34(12):2562–70.